# A Golden Section Search Algorithm Based Loss Minimization for Induction Motor Drive

Kirti Rai, Subodh Behari Lal Seksena, and Amarnath Thakur

Electrical and Electronics Engineering
National Institute of Technology, Jamshedpur, India
kirtisinha2809@yahoo.in

*Abstract*: The present manuscript proposes a loss model controller (LMC) based on the Golden Section Search (GSS) algorithm for efficiency optimization of induction motor (IM) drives. The vector controlled or field-orientated induction motor (IM) drive system operates at rated flux in all the speed range. Even at low load, where the flux demand for IM operation is low, the drive is operated at rated flux and thus, unnecessarily energy is wasted. Therefore, to overcome this problem, the proposed algorithm searches for the optimal reference value of flux component of current ( $i_{ds}$ ) for which the electrical input power of the system should be minimal. The search algorithm is very fast and the algorithm has no effect on parameter variation and also no additional hardware machinery for hardware implementation is required. In addition, it does not require the knowledge of speed and torque in the searching process, and is insensitive to motor parameter variations. The simulation results for various speed patterns and operating conditions are presented in this paper. Stability study of the whole drive system is also carried out utilizing the optimizing scheme. The simulation results demonstrate the effectiveness of the proposed algorithm and also the experimental validation of same on dSPACE-1104 based laboratory prototype has confirmed the robustness of the proposed algorithm in terms of optimal efficiency.

*Keywords:* AC motor drives, Induction motor drives, Estimation, Optimization, Losses Minimization, Golden Section Search (GSS).

NOMENCLATURE

| | |
|---|---|
| $v_s, v_s$ | : stator and rotor voltages (V) |
| $v_{ds}, v_{qs}$ | : d and q-axis components of stator voltage (V) |
| $i_{ds}, i_{qs}, i_{dr}, i_{qr}$ | : d and q-axis components of stator and rotor current (A) |
| $\psi_{ds}, \psi_{qs}, \psi_{dr}, \psi_{qr}$ | : d and q-axis components of stator and rotor flux (Wb) |
| $\psi_{dm}, \psi_{qm}$ | : d and q-axis components of mutual flux (Wb) |
| $L_s, L_m, L_r$ | : stator, mutual and rotor inductances (H) |
| $R_s, R_r, R_{fe}$ | : stator, rotor, and iron loss resistance (Ω) |
| $i_0, i_{fe}, i_m$ | : no-load, iron loss, and magnetizing current (A) |
| $\omega_e, \omega_r$ | : synchronous speed, and rotor speed(rad/s) |
| $\sigma = 1 - L_m^2/(L_s L_r)$ | : total leakage factor |
| $T_r$ | : rotor circuit time constant (s) |
| $A, B, C$ | : matrices for state-space representation |
| $c_{ij}$ | : $(i, j)^{\text{th}}$ element of $adj(A)$ |
| ^, * | : estimated, reference quantity |
| $s$ | : stationary quantity |
| $p$ | : time-derivative operator |

Received: April 14th, 2018. Accepted: March 16th, 2019
DOI: 10.15676/ijeei.2019.11.1.9

## 1. Introduction

Induction motors specially squirrel-cage type are widely used in industries because of robustness, good power/mass relation, low cost and easy maintenance throughout its life cycle. IMs are easy to maintain due to their simple structure, reliability, high efficiency, and low cost. The distinction of IM has led to its global increase in sales of up to 85 percent in electrical motors [1] [2] [3]. However, more than half of the electric energy consumed by industrial facilities is due to the use of induction motors. With the massive use of induction motors, electrical energy consumption has increased exponentially over the years. They have a low power factor at partial load if operated at rated flux, hence poor efficiency causes wastage of energy, increased operational cost and leads to significant loss of revenue if run for long durations. Because of the huge number ofunits operating worldwide, even a minute efficiency improvement may lead to significant environmental and economic contributions.

In high dynamic performances, control schemes used in industrial applications like vector control and direct torque control, the flux is usually maintained constant equal to its nominal value; in this situation the induction motor runs efficiently around the nominal operating point [2], [3]. When the load is reduced considerably, the losses are greatly increased and the electrical energy consumption is then highly affected [3-6]. Energy saving in induction motor drives aims at controlling the motor to match the load requirement but with minimum loss. So far, many approaches have been developed in order to obtain a highly efficient IM drives. It is one of the most attractive and active subjects in the field of motion control. The techniques allowing efficiency improvement can be divided into two categories. The first category is so called loss model controllers (LMC) and the second one is the search controllers approach (SC) [4], [5].

The SCs offers the advantage to be robust against the parameters variation but have a very sluggish response whereas the LMCs are very fast but parameters dependent. In other hand the LMCs to be accurate. The model that will be used to drive the LMC algorithm must be extended to include all the loss components, such as: iron loss, copper loss, stray load loss, etc. this problem might be tackled, if necessary using online optimization algorithm.

In last few decades, huge efforts are put forward by both developed and developing countries in the line of energy-saving. The electric motors are the largest consumer of total electricity produced globally (nearly 65-70%) [6], [7]. Precisely, out of this share of percentage, the three-phase induction motors (IMs) of different capacities (ranging from few Hp to 100 Hp) utilizes approximately 85- 90% of this electricity. Moreover, The IM drives have an annual expansion rate of 1.5% in industrial sector and 2.2% in tertiary sector for electricity consumption [8]. Since, a huge quantity of IM drive are operational worldwide and every year there is definite positive increase in their numbers, even a small improvement in efficiency by minimizing the losses will significantly have a good impact on saving of revenue, fuel consumption and other associated factors [9]. According to the reports available, every 1% improvement in motor efficiency might lead to savings of over $1 billion per annum in energy prices, the consumption of coal is reduced by5.4-9.1 million tons per annum and further bringing down greenhouse emission by nearly 13.6-18.1 million tons [10].

Minimization of loss in the induction motor is directly related to the choice of the flux level. But extreme minimization causes a high copper loss [11]. For constant speed operation, if torque is variable then flux have to vary, to improve the drive efficiency. A number of energy optimization strategies such as simple state control [12], search control [13] and loss model based control [14] for IM drive are found in the literature. The loss model based control consists of computing losses by using the machine model and selecting a flux level that can be used to minimize the losses. The second category is the power-measure-based approach, also known as search controllers (SCs), in which the flux is decreased until the electrical input power settles down to the lowest values for a given torque and speed [15], [16], [17].

In the present work, GSS based algorithms are used to minimize the drive loss for IM. A performance analysis of the IM drive system is carried out using GSS based algorithm in different operating conditions. The drive system consists of an energy optimization algorithm

based on the power loss of drive and speed error signal to generate optimal value of $i_{ds}^*$ and hence optimal rotor flux.

The paper is organized in seven sections. In section-2, the loss minimization scheme for IM is discussed. Section-3 discusses the GSS method concept and energy optimization techniques for IM drive. The measurement of input power is discussed in Section-4. Section-5 briefly explains the implementation of the GSS algorithm for loss minimization of the IM drive system. The system stability analysis using Bode plots are detailed in section-6. Simulation results are presented in section-7. Section-8 includes the experimental validation of simulation results. Finally, section-9 concludes the work carried out.

## 2. Loss Minimization Mechanism

The loss minimization algorithm is based on searching optimal value of the flux component of stator current $(i_{ds})$, for which the input power of the system can be minimal. The input power can be calculated as the product of the measured DC voltage $(V_{dc})$ and DC current $(I_{dc})$ as follow:

$$P_{in} = V_{dc} \bullet I_{dc} \tag{1}$$

The efficiency of machine can be defined as the ratio of the mechanical output power to the electrical input power. Therefore, for increasing the efficiency of a machine, the electrical input power can be optimized to reduced value by minimizing the total losses. Thus, the loss minimization can be accomplished by adjusting the flux level through the reference flux component current $(i_{ds}^*)$. For the generation of reference flux current, the techniques for the loss minimization is divided into two categories [18]. The first category is called as loss-model based approach [18], [19], [20], [21]. In this method, the loss is computed by using the machine model and selecting the flux level that minimizes the losses. The second method is power based approach, known as search controllers (SC), in which the flux is decreased until the electrical input power is minimized to the optimal lowest level. SCs offers optimum efficiency based on the exact measurement of power input and is independent of the machine parameters [22], [23], [24].

## 3. Golden Section Search Algorithm

In GSS based algorithm, the maximum value of the flux current equal to its rated value $(i_{dsmax} = i_{ds})$ is defined and the minimal value equal to $\alpha * i_{ds}$, where $\alpha =$ (~0.5) depending on load levels. The algorithm calculates the flux current in the interval between $(i_{dsmin}, i_{dsmax})$ which is fed to the control system to reduce the total input power of the drive. The input power is calculated in (1).

The new values of the reference flux current $(i_{ds})$ are calculated using two golden sections $F_1$ and $F_2$ calculated as:

$$F_1 = \frac{\sqrt{5}-1}{2} = 0.618 \text{ and } F_2 = \frac{3-\sqrt{5}}{2} = 0.382 \tag{2}$$

The algorithm calculates two values of the reference flux current $(i_{ds1}^*, i_{ds2}^*)$ in the interval $(i_{dsmin}, i_{dsmax})$ using golden sections. The input power corresponding to these two currents levels are calculated as $P(i_{ds1}^*), P(i_{ds2}^*)$ as depicted in (1). The reference flux current $(i_{ds1}^*, i_{ds2}^*)$ consequently re-calculated and their corresponding values of input power are re-measured and re-evaluated. The search procedure repeats itself until the desired accuracy is met.

$$\left| i_{ds2}^{*} - i_{ds1}^{*} \right| < \varepsilon_i \tag{3}$$

where $\varepsilon_i$ is the flux current tolerance. The reference flux current final value is calculated by averaging the values of $i_{ds1}^{*}, i_{ds2}^{*}$ a

$$i_{ds}^{*} = \frac{i_{ds1}^{*} + i_{ds2}^{*}}{2} \tag{4}$$

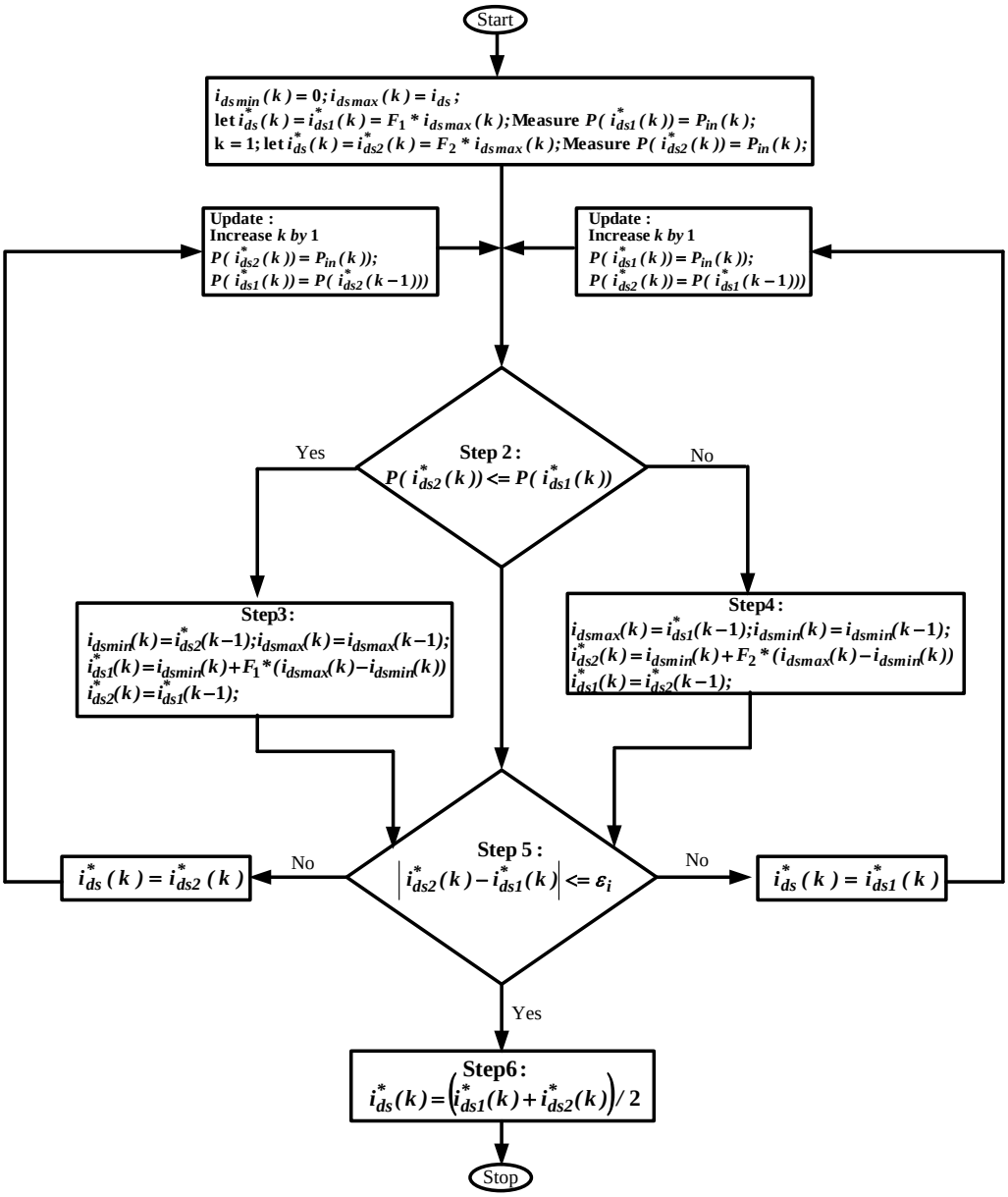


Figure 1. Flowchart of loss minimization by GSS

The complete implementation process of GSS algorithm is depicted in flowchart (Figure. 1). The GSS algorithm is fast insensitive to motor parameter variations. The technique comprises of all the losses including the loss in inverter, since the power entering to the system is measured and used in the optimization algorithm.

*A. Loss Model of Induction Motor*

The IM drive model with iron loss (Figure. 2) is given by following equations as [23], [25]:

$$v_{ds}^{s} = R_s i_{ds}^{s} + \sigma L_s p i_{ds}^{s} + L_m p i_{dm}^{s} - \omega_e \left(\sigma L_s i_{qs}^{s} + L_m i_{qm}^{s}\right) \tag{5}$$

$$v_{qs}^{s} = R_s i_{qs}^{s} + \sigma L_s p i_{qs}^{s} + L_m p i_{dm}^{s} + \omega_e \left(\sigma L_s i_{ds}^{s} + L_m i_{dm}^{s}\right) \tag{7}$$

$$v_{dr}^{s} = R_r i_{dr}^{s} + \sigma L_r p i_{dr}^{s} + L_m p i_{dm}^{s} - \left(\omega_e - \omega_r\right)\left(\sigma L_r i_{qr}^{s} + L_m i_{qm}^{s}\right) \tag{8}$$

$$v_{qr}^{s} = R_r i_{qr}^{s} + \sigma L_r p i_{qr}^{s} + L_m p i_{qm}^{s} + \left(\omega_e - \omega_r\right)\left(\sigma L_r i_{dr}^{s} + L_m i_{dm}^{s}\right) \tag{9}$$

The d- and q-axis components of magnetic flux are given by

$$\psi_{ds}^{s} = \sigma L_s i_{ds}^{s} + L_m i_{dm}^{s} \tag{10}$$

$$\psi_{qs}^{s} = \sigma L_s i_{qs}^{s} + L_m i_{qm}^{s} \tag{11}$$

$$\psi_{dr}^{s} = \sigma L_r i_{dr}^{s} + L_m i_{dm}^{s} \tag{12}$$

$$\psi_{qr}^{s} = \sigma L_r i_{qr}^{s} + L_m i_{qm}^{s} \tag{13}$$

The induced voltage on the magnetizing branch is given as

$$v_{di}^{s} = L_m p i_{dm}^{s} - \omega_e L_m i_{dm}^{s} \tag{14}$$

$$v_{qi}^{s} = L_m p i_{qm}^{s} + \omega_e L_m i_{qm}^{s} \tag{15}$$

The interaction between stator current and magnetic flux components give electromagnetic torque in d-q coordinate frame as

$$T_{em} = \frac{3}{2} P \frac{L_m}{\sigma L_{r+L_m}} \left[\psi_{qr}^{s}\left(i_{ds}^{s} - i_{dfe}^{s}\right) - \psi_{dr}^{s}\left(i_{qs}^{s} - i_{qfe}^{s}\right)\right] \tag{16}$$

The total loss is given by

$$P_{loss} = \frac{3}{2}\left[R_s\left(i_{ds}^{s} + i_{qs}^{s}\right) + R_r\left(i_{ds}^{s} + i_{qs}^{s}\right) + \frac{1}{R_f}\left(v_{di}^{s} + v_{qi}^{s}\right)\right] \tag{17}$$

Or, $P_{loss} = P_{js} + P_{jr} + P_{fe}$ (18)

Where, $P_{js}$ = stator copper loss; $P_{jr}$ = rotor copper loss; $P_{fe}$ = core loss including eddy current and hysteresis loss.

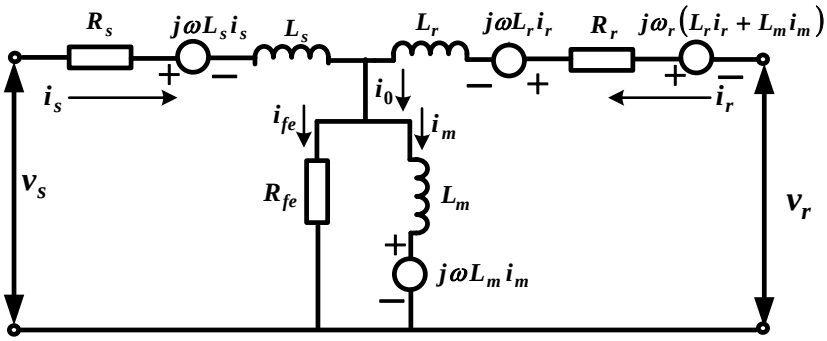


Figure 2. Equivalent circuit model of the induction motor in T-form with iron loss.

## 4. Input power measurement

The drive is equipped with DC voltage and current sensors to evaluate *P*in accurately. The motor is run in closed loop speed control without load such that the contribution of the rotor copper losses is negligible.

The currents, voltages and input powers are recorded when steady-state conditions are reached.

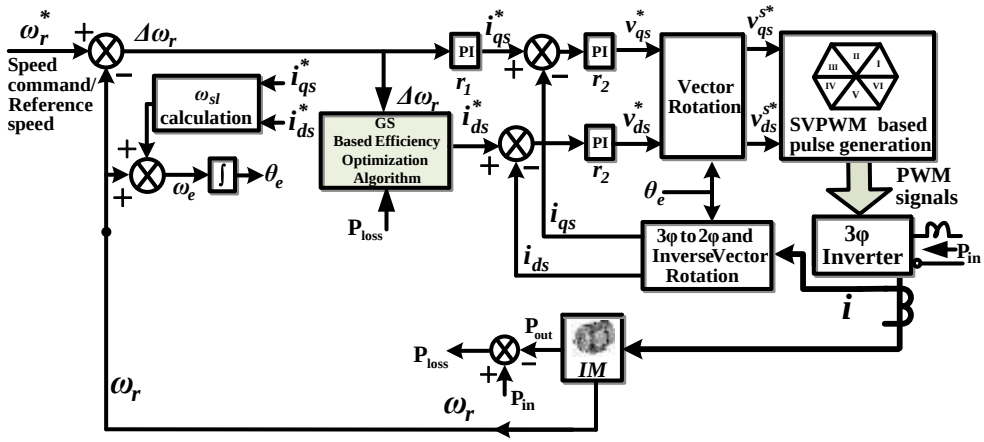


Figure. 3. Schematic diagram of vector controlled IM drive and efficiency optimization scheme.

## 5. Loss Minimization of IM Drive

The improved dynamic performance with minimum loss is the important requirements for IM drive. Therefore, loss minimization schemes using GSS algorithm [26] have been incorporated separately in the outer loop of the control scheme. The vector control not only has the advantage of excellent dynamic performance, but also, enables decoupled control of torque and flux through d-axis (flux-producing) and q-axis (torque-producing) currents in the steady state. This makes the inclusion of the loss minimization algorithm very simple [27]. However, the present energy optimization algorithm using golden section technique for IM drive is based on power loss of the drive system. The drive loss is calculated from the difference between the power input to the inverter and the shaft power output. The reference flux current, $i_{ds}^*$ is generated by the optimization algorithm, while the torque component of current is acquired from the speed control loop. In the transient state, when either the speed command or the load torque is changed, the nominal value of the $i_{ds}^*$ comes into play. The transient speed is easily detected when the speed error signal ($\Delta\omega_e$) reaches the maximum value 0.5 rad/s and the energy

optimization algorithm starts settling the $i_{ds}^*$ to the required optimal value. The optimal value of $i_{ds}^*$ generates the optimized required flux without affecting the output power. The optimal value of flux reduces the power loss of the drive system thus fulfilling objective of proposed work. The complete schematic diagram for estimation of speed with loss minimization algorithm is shown in Figure. 3.

## 6. System stability Analysis

To carry out the stability analysis of any system, the variables must be time-invariant [11]. The IM model in synchronously rotating $(\omega_e)$ reference frame has been expressed as

$$\begin{bmatrix} \dot{i}_{ds} \\ \dot{i}_{qs} \\ \dot{\psi}_{dr} \\ \dot{\psi}_{qr} \end{bmatrix} = \underbrace{\begin{bmatrix} -p_1 & \omega_e & p_2 & p_3\omega_r \\ -\omega_e & -p_1 & -p_3\omega_r & p_2 \\ p_4 & 0 & -p_5 & \omega_{sl} \\ 0 & p_4 & -\omega_{sl} & -p_5 \end{bmatrix}}_{A} \begin{bmatrix} i_{ds} \\ i_{qs} \\ \psi_{dr} \\ \psi_{qr} \end{bmatrix} + \frac{1}{\sigma L_s} \underbrace{\begin{bmatrix} 1 & 0 \\ 0 & 1 \\ 0 & 0 \\ 0 & 0 \end{bmatrix}}_{B} \begin{bmatrix} v_{ds} \\ v_{qs} \end{bmatrix} \tag{19}$$

$$\begin{bmatrix} i_{ds} \\ i_{qs} \end{bmatrix} = \underbrace{\begin{bmatrix} 1 & 0 & 0 & 0 \\ 0 & 1 & 0 & 0 \end{bmatrix}}_{C} \begin{bmatrix} i_{ds} \\ i_{qs} \\ \psi_{dr} \\ \psi_{qr} \end{bmatrix} \tag{20}$$

where, $p_1 = \frac{1}{\sigma L_s}\left(R_s + \frac{L_m^2}{L_r \tau_r}\right)$, $p_2 = \frac{1}{\sigma L_s}\left(R_s + \frac{L_m}{L_r \tau_r}\right)$, $p_3 = \frac{1}{\sigma L_s}\left(\frac{L_m}{L_r}\right)$, $p_4 = \left(\frac{L_m}{\tau_r}\right)$ and $p_5 = \left(\frac{1}{\tau_r}\right)$

In the state space domain, (19-20) can be represented as

$$\dot{x} = Ax + Bu \tag{21}$$

$$y = Cx \tag{22}$$

where, $A$, $B$, $C$ are obtained from (19)-(20) and $x = [i_{ds} \quad i_{qs} \quad \psi_{dr} \quad \psi_{qr}]^T$, $u = [v_{ds} \quad v_{qs}]^T$, $y = [i_{ds} \quad i_{qs}]^T$

Linearizing the state space equation around a stable operating point say $x_0$, the small signal representation is as

$$\Delta \dot{x} = A\Delta x + \Delta A x_0 \tag{23}$$

$$\Delta y = C\Delta x \tag{24}$$

$$\text{or, } \Delta y = C(sI - A)^{-1}\Delta A\, x_0 \tag{25}$$

$x_0 = [i_{ds0} \;\; i_{qs0} \;\; \psi_{dr0} \;\; \psi_{qr0}]^T$ represents the operating point.

For checking the feasibility of the algorithm for rotor speed estimation, $\Delta A$ is calculated in terms of $\Delta\omega_r$ as;

$$\Delta A = \begin{bmatrix} 0 & 0 & 0 & p_3 \\ 0 & 0 & -p_3 & 0 \\ 0 & 0 & 0 & -1 \\ 0 & 0 & 1 & 0 \end{bmatrix} \Delta\omega_r \tag{26}$$

$$C = \begin{bmatrix} 1 & 0 & 0 & 0 \\ 0 & 1 & 0 & 0 \end{bmatrix} \tag{27}$$

Using 20 and 26, the expression of $\Delta y$ in 25 becomes;

$$\Delta y = \begin{bmatrix} \Delta i_{ds} \\ \Delta i_{qs} \end{bmatrix} = \begin{bmatrix} 1 & 0 & 0 & 0 \\ 0 & 1 & 0 & 0 \end{bmatrix} (sI - A)^{-1} \begin{bmatrix} 0 & 0 & 0 & p_3 \\ 0 & 0 & -p_3 & 0 \\ 0 & 0 & 0 & -1 \\ 0 & 0 & 1 & 0 \end{bmatrix} \begin{bmatrix} i_{ds0} \\ i_{qs0} \\ \psi_{dr0} \\ \psi_{qr0} \end{bmatrix} \Delta\omega_r \tag{28}$$

$$\text{Let, } (sI - A)^{-1} = \begin{bmatrix} c_{11} & c_{12} & c_{13} & c_{14} \\ c_{21} & c_{22} & c_{23} & c_{24} \\ c_{31} & c_{32} & c_{33} & c_{34} \\ c_{41} & c_{42} & c_{43} & c_{44} \end{bmatrix} \tag{29}$$

The transfer function of $\frac{\Delta i_{ds}}{\Delta\omega_r}$ and $\frac{\Delta i_{qs}}{\Delta\omega_r}$ obtained from 28 can be represented as

$$\frac{\Delta i_{ds}}{\Delta\omega_r} = \frac{(c_{14} - p_3 c_{12})\psi_{dr0}}{|sI - A|} \tag{30}$$

$$\frac{\Delta i_{qs}}{\Delta\omega_r} = \frac{(c_{24} - p_3 c_{22})\psi_{dr0}}{|sI - A|} \tag{31}$$

where, $a\mathrm{dj}(sI - A) = [C_{ij}]$ and $i, j$ varies from 1 to 4.

From Figure 3, the following expressions have been derived:

$$v_{ds}^* = \left(k_{p3} + \frac{k_{i3}}{s}\right) \times \left(i_{ds}^* - i_{ds}\right) = r_2\left(i_{ds}^* - i_{ds}\right) \tag{32}$$

$$v_{qs}^* = \left(k_{p2} + \frac{k_{i2}}{s}\right)\left\{\left(k_{p1} + \frac{k_{i1}}{s}\right) \times \left(\omega_r^* - \omega_r\right) - i_{qs}\right\} = r_2\left\{r_1\left(\omega_r^* - \omega_r\right) - i_{qs}\right\} \tag{33}$$

where, $r_1 = \left(k_{p1} + \frac{k_{i1}}{s}\right) =$ transfer function of the speed PI controller, $r_2 = \left(k_{p2} + \frac{k_{i2}}{s}\right) =$ transfer function of current PI controllers, as seen from Figure 4.

To check feasibility of the algorithm for speed estimation, $\Delta A$ is calculated in terms of $\Delta\omega_r$ with an aim of obtaining $\Delta i_{ds}/\Delta\omega_r$ and $\Delta i_{qs}/\Delta\omega_r$. From the small signal error equation,, $\Delta\varepsilon/\Delta\hat{\omega}_r$ is represented as:

$$\frac{\Delta\varepsilon}{\Delta\hat{\omega}_r} = k_2\frac{\Delta i_{ds}}{\Delta\omega_r} + k_3\frac{\Delta i_{ds}}{\Delta\omega_r} + (k_5 - k_4) = G(s) \tag{34}$$

where, $k_2 = v_{qs0} - 2\sigma L_s\omega_{e0}i_{ds0} - 2\omega_{e0}\frac{L_m^2}{L_r}i_{ds0} + r_2 i_{qs0}$; $k_3 = -v_{ds0} - 2\sigma L_s\omega_{e0}i_{qs0} - r_2 i_{ds0}$;

$k_4 = -\sigma L_s i_{ds0}^2 - \sigma L_s i_{qs0}^2 - \frac{L_m^2}{L_r}i_{ds0}^2$; $k_5 = -\sigma L_s i_{ds0}^2 - \sigma L_s i_{qs0}^2 - \frac{L_m^2}{L_r}i_{ds0}^2 - r_1 r_2 i_{ds0}$;

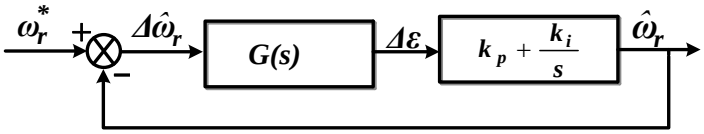


Figure 4. Closed loop representation of speed estimator

The closed loop transfer function representation (Figure 4) of the speed estimator is obtained as:

$$\frac{\hat{\omega}_r}{\omega_r^*} = G(s)\left(k_p + \frac{k_i}{s}\right) \Big/ \left(1 + G(s)\left(k_p + \frac{k_i}{s}\right)\right) \tag{35}$$

where, $\left(k_p + \frac{k_i}{s}\right)$ = is the transfer function of the PI controller.

Using (35), the stability analysis using linearized machine equations for the whole IM drive system based on GSS algorithm are carried out for both motoring and regenerating modes of operation. The IM drive system based on GSS algorithm is found to be stable in motoring mode (Figure. 5(a)), as well as in regenerating mode of operation (Figure. 5(b)) as confirmed in the relevant bode plots. It can be observed from the plots that all poles and zeroes are lying in the left hand side of the s-plane. This confirms stability of the IM drive operation based on GSS algorithm in both the modes.

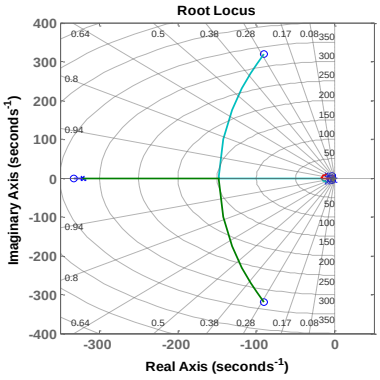


(a)

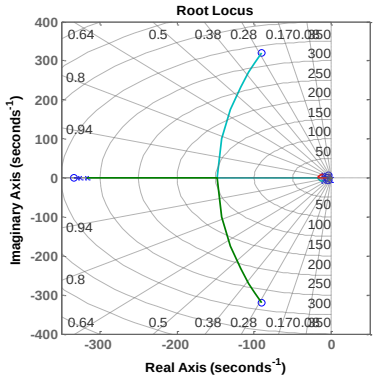


(b)

Figure 5. Stability analysis using Root locus plot for the IM drive system for $R_r = 4.01\ \Omega$ and $R_s = 5.55\ \Omega$ utilizing GSS algorithm in: (a) motoring mode ($\omega_r = 10$ rad/s and $T_L = 5$ Nm) and (b) in regenerating mode ($\omega_r = 10$ rad/s and $T_L = -5$ Nm).

## 7. Simulation Results

The performance of the proposed GSS algorithm for loss minimization of vector controlled IM drive is verified in Matlab/Simulink for various test cases as follows. The simulation results show the speed, rotor flux, stator current, and IM drive's loss responses before and after the optimization schemes are initiated for IM drive. The details specification of the 3-phase, 1.5 kW IM drive is given in APPENDIX A.

*A. Step change in rotor speed*

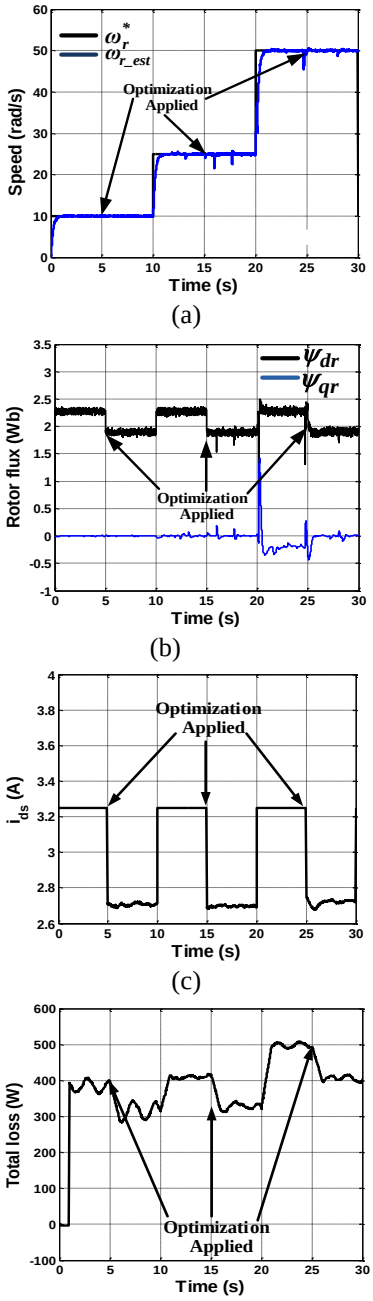


Figure 6. Simulation results of the IM drive with GSS scheme for step change in rotor speed at 5 Nm load torque: (a) reference, estimated and actual speeds, (b) d- and q-axis rotor flux, (c) d-axis stator current, and (d) total loss of the drive.

The simulation results of GSS based optimization scheme for IM drive is studied in the motoring mode by a step change in the reference speed as shown in Figure. 6. An increasing step change in the speed command is applied at every 10 s and the reference and actual speeds are shown for the whole speed range in Figure. 6(a) for GSS based optimization algorithm. Throughout the operation a constant torque of 5 Nm is maintained. The flux component of the

stator current ( $i_{ds}$ ) is shown in Figure. 6(b). After every speed transient period, $i_{ds}$ is adjusted to the optimal value by GSS algorithm. The flux orientation is also altered as the $i_{ds}$ changes and is shown in Figure. 6(c). The loss of the IM drive system is shown in Figure. 6(d). It can be observed that without the efficiency optimization algorithm in the transient period, the drive loss is on the higher side as compared to the duration after optimization algorithm becomes functional.

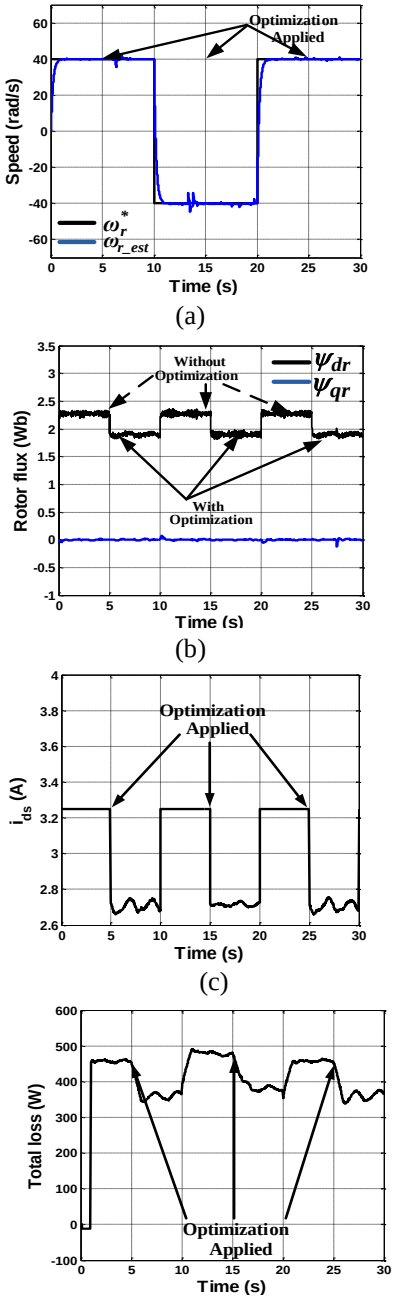


Figure. 7. Simulation results of IM drive with GSS scheme for second quadrant operation at 5 Nm load torque: (a) reference, estimated and actual speeds, (b) d- and q-axis rotor flux, (c) d-axis stator current, and (d) total drive's loss.

*B. Regenerative mode operation: Second quadrant operation*

Table 1. Performance Assessment of IM drive operation in motoring and regenerating mode with and without GSS based optimization.

| Speed (rad/s) | Torque (Nm) | Loss (W), with Conventional optimization | Loss (W), with GSS optimization |
|---|---|---|---|
| 50 | 5 | 485 | 460 |
| 40 | | 423 | 403 |
| 30 | | 396 | 383 |
| 20 | | 364 | 355 |
| 10 | | 341 | 331 |
| 5 | | 327 | 311 |
| 0 | | 318 | 298 |
| 0 | -5 | 322 | 306 |
| 5 | | 331 | 319 |
| 10 | | 350 | 341 |
| 20 | | 363 | 353 |
| 30 | | 388 | 371 |
| 40 | | 431 | 422 |
| 50 | | 472 | 460 |

The performance of the IM drive system in second quadrant is shown in Figure. 7 shows the transition of the estimator from motoring mode and back keeping the load torque constant at 5 Nm. The estimated speed follows the actual speed satisfactorily (Figure.7(a)) for GSS loss optimization scheme. The optimization algorithm comes into play at 5 s, 15 s, and 25 s. The optimal and non-optimal fluxes are shown in Figure. 7(b) for GSS optimization scheme. The change in current during the entire time period is shown in Figure.7(c). The decrement in loss based on GSS optimization is shown in Figure.7(d). It can be observed from the results that GSS based optimization scheme is more efficient in reducing the loss than drive without GSS scheme. A quantitate performance of the IM drive with loss minimization schemes are presented in tabular form for different speed ranges at 5 Nm load torque in Table I. The Table summarizes the results of loss minimization achieved by GSS optimization scheme for IM drive.

## 8. Experimental Validation

A laboratory prototype is developed to validate the performance of the proposed loss minimization using dSPACE-1104. A representative block diagram of the experimental setup for GSS based loss minimization schemes for IM drive is shown in Figure. 3. The code of the proposed estimator for dSPACE-1104 controller is generated with 10 kHz sampling frequency at 4.7 kHz inverter switching rate using MATLAB/Simulink interface. The stator windings are fed through a space-vector pulse width modulated (SVPWM) inverter operating with a switching frequency of 4.7 kHz for the control purpose. The control pulses for the inverter are generated according to the proposed algorithm and field orientation. Two current sensors are employed to sense the line currents for the execution of the proposed control scheme in dSPACE-1104 controller board which has built-in analog-to-digital converter (ADC), digital-to-analog converter (DAC) and dedicated Input/Output (I/O) ports. A few results of drive's operation are presented in the following subsections.

*A. Step Change of Rotor Speed*

The experimental results corresponding to the simulation results of the IM drive system is shown in Figure. 8 for GSS based loss minimization scheme. The step change in the reference

speed is considered as shown in Figure. 8(a). The d- axis and q- axis rotor flux is depicted in Figure. 8(b). Figure. 8(c) shows the flux components of the stator current ( $i_{ds}$ ) for GSS based algorithm. After every speed transient period, $i_{ds}$ is adjusted to the optimal value by GSS algorithm. The loss of the IM drive shown in Figure. 8(d) for GSS based scheme. It can be observed that for GSS based loss minimization scheme, the drive loss is minimized in the transient period as compared to the period without GSS based optimization scheme. Throughout the operation a constant load torque of 5 Nm is maintained.

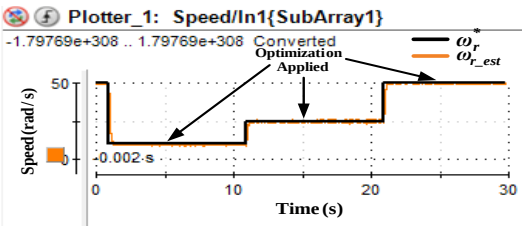


(a)

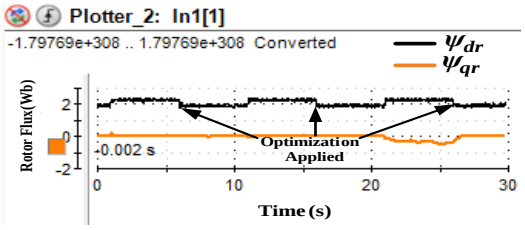


(b)

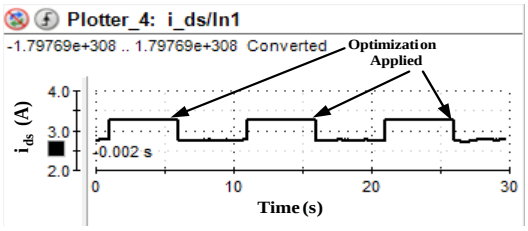


(c)

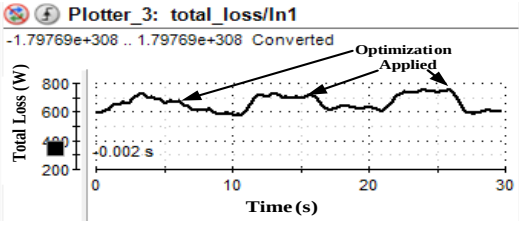


(d)

Figure 8. Experimental results of IM drive with GSS scheme for step change in rotor speed at 5 Nm load torque: (a) reference, estimated and actual speeds, (b) d- and q-axis rotor flux, (c) d-axis stator current, and (d) total loss of the drive

*B. Regenerative mode operation: Second quadrant operation*

The experimental results for GSS based loss minimization scheme in both the motoring and regenerating modes of operation is presented in Figure. 9. In the motoring (1st quadrant) and regenerating (2nd quadrant) modes, the load torque is kept constant at 5 Nm while the reference

speed is reversed alternatively at +40 rad/s and -40 rad/s after every 10 s (Figure. 9(a)). The estimated speed is found to track the reference speed satisfactorily. The energy optimization algorithm is initiated at 5 s, 15 s, and 25 s respectively, thus, reducing the d-axis rotor flux to an optimized value (Figure 9(b)). Figure 9(c) signifies the optimized d-axis stator current waveform for the aforesaid scheme. The total losses of the IM drive before and after the optimization algorithm is functional is shown in Figure 9(d). It can be observed from the results that the performance of GSS based loss minimization scheme for IM drive surpasses performance of IM drive without GSS based algorithm.

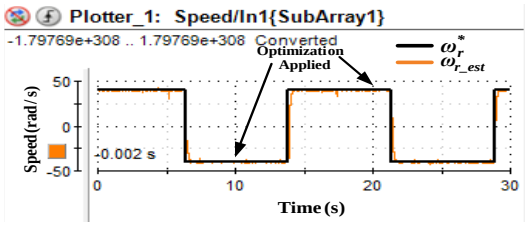


(a)

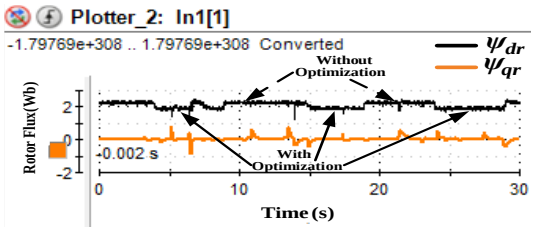


(b)

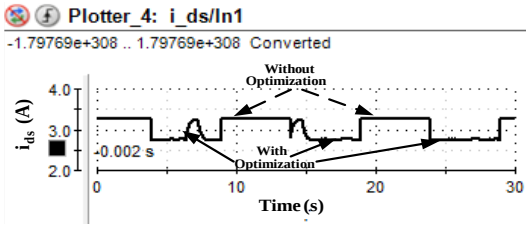


(c)

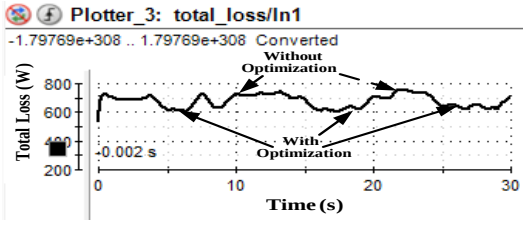


(d)

Figure. 9. Experimental results of IM drive with GSS scheme for second quadrant operation at 5 Nm load torque: (a) reference, estimated and actual speeds, (b) d- and q-axis rotor flux, (c) d-axis stator current, and (d) total drive's loss.

## 9. Conclusion

This paper presents a loss minimization scheme for IM drive known as GSS (GSS) method. The loss-minimization algorithm is developed considering the drive's loss for the scheme. The performance of the IM drive system based on the GSS algorithm has been verified in both

simulation and experiment at different operating conditions. Moreover, the stability analysis of the IM drive system in the motoring and regenerating modes of operation confirms a stable drive operation for the scheme. The GSS based scheme for IM drive has been implemented in real time for a laboratory 1.5 kW motor using d-SPACE controller board DS1104. The efficiency optimization algorithm generates the optimal value of $i_{ds}^{*}$ minimizing the core loss of the drive system as the flux level is highly optimized. It is established from the results that the performance of the IM drive with the GSS based optimization algorithm remarkably reduces the loss of drive system as compared to results obtained without GSS based optimization scheme.

## APPENDIX A

### A.1. MACHINE RATING AND PARAMETERS

| | |
|---|---|
| Rated shaft power $(P_r)$ | 1.5 kW |
| Line-to-line voltage $(v_{LL\ rms})$ | 415 V, 50 Hz |
| Poles $(P)$ | 4 |
| Magnetizing inductance $(L_m)$ | 0.7 H |
| Stator and rotor leakage inductance $(L_{ls} = L_{lr})$ | 0.0352 H |
| Stator resistance $(R_s)$ | 5.205 Ω |
| Rotor resistance $(R_r)$ | 4.075 Ω |

## 10. References


[1] A.Siddique, G.S.Yadava and B.Singh, " A review of stator fault monitoring techniques of induction motors," *IEEE Trans Energy Convers.*, vol. 20, pp. 106-114, 2005.

[2] S. Kashif, M. Saqib and S.Zia, "Implementing the induction-motor drive with four switch inverter: an application of neural networks," *Expert Syst Appl.*, vol. 38, pp. 137-148, 2011.

[3] T.H.dos.Santos, A.Goedtel, SAO.Silva and M.Suetake, "Scalar control of an induction motor using a neural sensorless technique," *Electric Power Systems Research*, vol. 108, pp. 322-330, 2014.

[4] J.Li, L.Xu and Z.Zhang, "A New Efficiency Optimization Method on Vector Control of Induction Motors," *IEEE International Conference on Electric Machines and Drives*, pp. 1-6, 2005.

[5] S.Ghozzi, K.Jelassi and X.Roboam, "Energy optimization of induction motor drives," *IEEE International Conference on Industrial Technology*, pp. 1-6, 2004.

[6] P. Choudhary, S. Dubey and V. Gupta, "Efficiency optimization of induction motor drive at steady-state condition," *International Conference on Control, Instrumentation, Communication and Computational Technologies (ICCICCT)*, Dec. 2015.

[7] Y.H.M.Yatim and W.M.Utomo, "To develop an efficient variable speed compressor motor system," *Universiti Teknologi Malaysia (UTM)*, 2007.

[8] R.Hanitsch, "Energy efficient electric motors," *World Climate & Energy Event*, pp. 45-50, Jan. 2002.

[9] Y.Yakhelet, "Energy efficiency optimization of induction motors," *Boumerdes University, Boumerdes, Algeria*, 2007.

[10] M.W.Turner, V.E.McCormick and J.G.Cleland, "Efficiency optimization control of AC induction motors: Initial laboratory results," *US Environmental Protection Agency, Research and Development.*, 1996.

[11] B. K. Bose, Modern power electronics and ac drives, New Delhi: *Prentice Hall*, 2002.

[12] M. E. H. Benbouzid and N. S. N. Said, "An efficiency-optimization controller for induction motor drives," *IEEE Power Engineering Review,* vol. 18, no. 5, pp. 63-64, 1998.

[13] D. S. Kirschen, D. W. Novotny and W. Suwanwissot, "Minimizing induction motor losses by excitation control in variable frequency drives," *IEEE Trans. Ind. Appl.,* Vols. IA-20, no. 5, pp. 1244-1250, 1984.

[14] R.P.Vieira, C.C.Gastaldini, R.Z.Azzolin and H.Grundling, "Sensorless sliding-mode rotor speed observer of induction machines based on magnetizing current estimation," *IEEE Trans. Ind. Electron.,* vol. 61, no. 9, pp. 4573-4582, Sept. 2014.

[15] J.Li, H.Ren, Q.Huang and Y.Zhong, "A novel on-line MRAS rotor resistance identification method insensitive to stator resistance for vector control systems of induction machines," in *IEEE Int. Symp. Ind. Electron.,* Bari, 2010.

[16] R.Wei and A.Gensior, "A model-based loss-reduction scheme for transient operation of induction machines," *18th European Conference on Power Electronics and Applications (EPE'16 ECCE Europe),* Sept. 2016.

[17] M.R.David, H.F.Hofmann and J.Sun, "Offline identification of induction machine parameters with core loss estimation using the stator current locus," *IEEE Transactions on Energy Conversion,* vol. 31, no. 4, pp. 1549-1558, 2016.

[18] A.Kusko and D.Galler, "Control means for minimization of losses in AC and DC drives," *IEEE Trans. Ind. App.,* Vols. IA-19, no. 4, pp. 561-570, 1983.

[19] R.D.Lorenz and S.M.Yang, "Efficiency-optimized flux trajectories for closed-cycle operation of field-orientation induction machine drives," *lEEE Trans.Ind. App.,* vol. 28, no. 3, pp. 574-580, 1992.

[20] G.0.Garcia, J.C.M.Luis, R.M.Stephan and E.H.Watanabe, "An efficient controller for an adjustable speed induction motor drive," *IEEE Trans.Ind. Electron.,* vol. 41, no. 5, pp. 533-539, 1994.

[21] G.C.D.Sousa, B.K.Bose and J.G.Cleland, "Fuzzy logic based on line efficiency optimization control of an indirect vector-controlled line efficiency optimization control of an indirect vector-controlled induction motor drive," *IEEE Trans. Ind. Electron.,* vol. 42, no. 2, pp. 192-198, 1995.

[22] D.S.Kirschen, D.W.Novotny and T.A.Lipo, "On-line efficiency optimization of a variable frequency induction motor drive," *IEEE Trans.Ind. Applicat.,* vol. 21, pp. 610-615, 1985.

[23] F.Zidani, M. E. H. Benbouzid and D. Diallo., "Fuzzy efficient-optimization controller for induction motor drive," *IEEE Power Engineering Review 20.10 (2000): 43-44.,* vol. 20, no. 10, pp. 43-44, 2000.

[24] J.C.Moreira, T.A.Lipo and V.Blasko, "Simple efficiency maximizer for an adjustable frequency induction motor drive," *IEEE Trans. Ind.Applicat.,* vol. 27, pp. 940-946, 1991.

[25] Z.Rouabah, F.Zidani and B.Abdelhadi, "Optimal efficiency of a fuzzy controller in a field oriented control induction motor drive," *4th International Conference on Electrical Engineering CEE06, Batna, Algeria,* pp. 135-138, Nov. 2007.

[26] S.S.Rao, Engineering Optimization: Theory and Practice, New York: John Wiley and Sons., 2009.

[27] C. M. Ta and Y. Hori, "Convergence improvement of efficiency-optimization control of induction motor drives," *IEEE Tran. Ind. Appl.,* vol. 37, no. 6, pp. 1746-1753, 2001.

**Keerti Rai** received B.Tech in Electrical and Electronics from LNCT Bhopal in the year 2005, M.Tech in Energy from NIT Bhopal in the year 2008. She has 4 years of teaching experience. Currently persuing PhD at Electrical and Electronics Department, NIT Jamshedpur. Hear research area includes electrical motor drive, energy saving in electrical motors.

**Subodh Behari Lal Seksena** was born in Gajraula (U.P.), India in 1951. He received the B.Sc, Electrical Engineering and M.Tech, Electrical Engineering with specialization in Power Systems from RIT Jamshedpur under Ranchi University Ranchi, India in 1974 & 1977, respectively and the Ph.D. Degree from University of ROORKEE, India ,in 1991. He is an recipient of Koshla Research Award in 1990, constituted by University of ROORKEE, for his research paper entiltled "A Self-Compensated Smart LVDT Transnducer", IEEE, Tr. on I & M, Vol- 38, No-3, June 1989. So far he has published over 62 research papers in International & National Journals and Conferences of repute. He had successfully supervised four Ph.D. Theses. Apart from that he has authored a book titled "Basic Electrical Engineering" published from Cambridge University Press, New Delhi, in 2016 & edited 04 nos. of technical titles on Electrical Engineering (Instrumentation & Measurement and Power Electronics) for McGraw Hill Publishers Company, New Delhi.

In 1977 he joined the Departement of Electrical Engineering, RIT Jamshedpur as a Lecturer. Having served the Departement/Institute for 39 years. He got retired under superannuation from there in April, 2016. Dr. Seksena is a Fellow Member of Institution of Engineers (India), Kolkata, FIE (I) 106487/4 EL & Life Member (LM 453) of Instrument Society of India, IISc. Campus, Bangalore. His research interests are Digital Instrumentation, Solid State Drives & Control, Power System, and Non-conventioal Energy Sources.

**Amarnath Thakur** received the B Sc (Engg.) degree in Electrical Engineering from MIT, Muzaffarpur, the M Tech degree from IIT(BHU), Varanasi and the Ph D degree from Department of Elecrical Engineering, IIT Kharagpur in 1979, 1982 and 1997 respectively. He is currently a Professor in the Department of Electrical and Electronics Engineering, National Institute of Technology Jamshedpur. His area of interest include power electronics and renewable energy system. He is life member of the Indian Society for Technical Education New Delhi and Institution of Engineers, India.